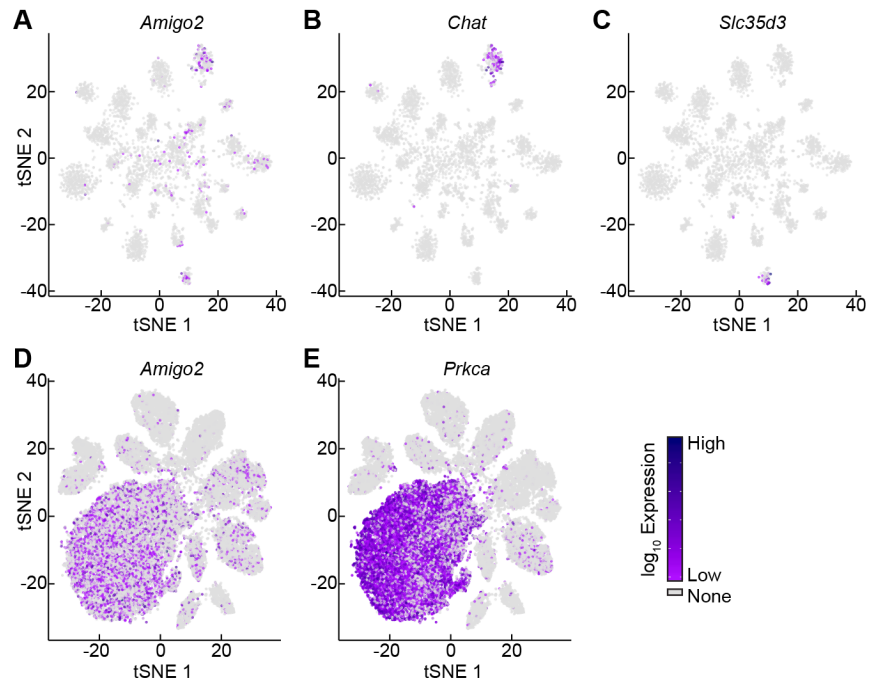


**Cell Reports, Volume 29**

**Supplemental Information**

**AMIGO2 Scales Dendrite Arbors in the Retina**

**Florentina Soto, Nai-Wen Tien, Anurag Goel, Lei Zhao, Philip A. Ruzycki, and Daniel Kerschensteiner**



**Figure S1. Expression of *Amigo2* in retinal single-cell RNA-Seq datasets** (related to Figure 1)

(A-C) tSNE dimension reduction of amacrine cell subtypes. All cells are plotted and color scale indicates (log<sub>10</sub>) normalized expression of *Amigo2* (A), *Chat* (B), and *Slc35d3* (C). Circles denote clusters with strong *Amigo2* expression in (A). Gray indicates zero expression.

(D-E) tSNE dimension reduction of bipolar cell subtypes. All cells are plotted and color scale indicates (log<sub>10</sub>) normalized expression of *Amigo2* (D) and *Prkca* (E). Gray indicates zero expression.

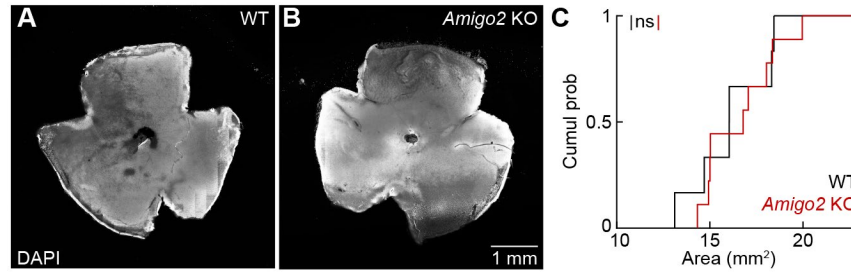


**Figure S2. Retinal area in wild-type and *Amigo2* KO mice** (related to Figure 2)

(A and B) Flat mount preparations of wild-type (A) and *Amigo2* KO retinas (P30) stained with DAPI.

(C) Cumulative distributions of the total areas of retinal flat mounts from wild-type ( $16.1 \pm 0.8 \text{ mm}^2$ ,  $n = 6$  retinas) and *Amigo2* KO ( $16.6 \pm 0.6 \text{ mm}^2$ ,  $n = 9$  retinas) mice.  $P = 0.78$  by Mann-Whitney U test.

For the statistical comparison in this figure, ns indicates no significant differences.

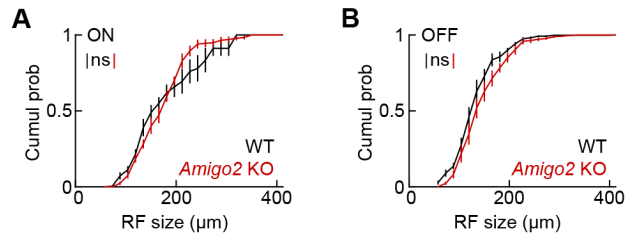


**Figure S3. The receptive field size of ganglion cells in wild-type and *Amigo2* KO mice** (related to Figure 6)

(A and B) Cumulative distributions of receptive field sizes measured from spike-triggered stimulus averages of ON (A) and OFF (B) ganglion cells during white noise stimulation. Receptive field sizes of ON (wild-type:  $n = 143$  cells,  $n = 5$  retinas, *Amigo2* KO:  $n = 156$  cells,  $n = 6$  retinas,  $P = 0.18$  by bootstrapping) and OFF ON (wild-type:  $n = 162$  cells,  $n = 5$  retinas, *Amigo2* KO:  $n = 233$  cells,  $n = 6$  retinas,  $P = 0.19$ ) ganglion cells were not significantly different between *Amigo2* KO and wild-type retinas.

Throughout the figure, ns indicates no significant differences for statistical comparisons.

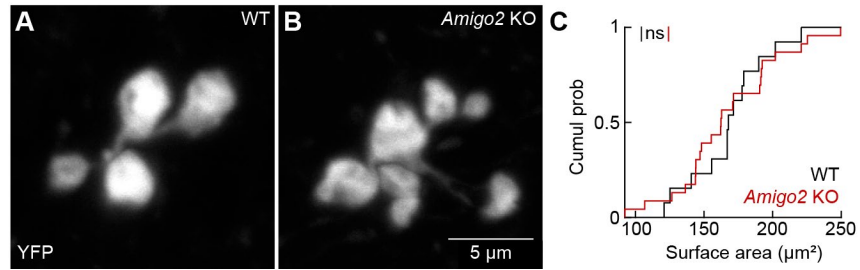


**Figure S4. RBC axon territories in wild-type and *Amigo2* KO mice** (related to Figure 7)

(A and B) Maximum intensity projections of RBC axons labeled by *AAV-Grm6-YFP* in wild-type (A) or *Amigo2* KO (B) retinas.

(C) Cumulative distributions of surface areas of RBC axon arbors in wild-type ( $168.1 \pm 7.9 \mu\text{m}^2$ ,  $n = 13$  cells,  $n = 5$  retinas) and *Amigo2* KO ( $166.8 \pm 7.8 \mu\text{m}^2$ ,  $n = 23$  cells,  $n = 4$  retinas) mice.  $P = 0.83$  by Mann-Whitney U test.

For the statistical comparison in this figure, ns indicates no significant differences.

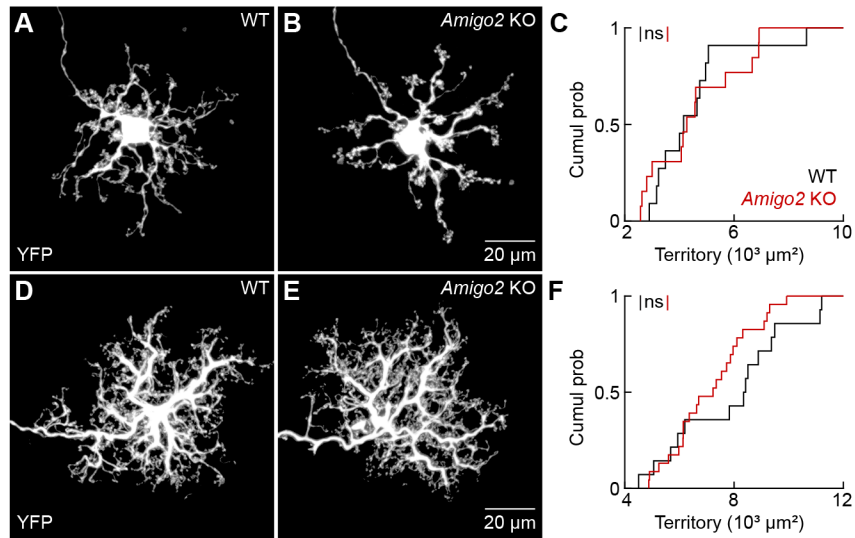


**Figure S5. Horizontal cell dendrites and axons in wild-type and *Amigo2* KO mice (related to Figure 7)**

(A and B) Maximum intensity projections of dendrites of horizontal cells labeled by AAV-CAG-YFP in wild-type (A) and *Amigo2* KO (B) mice.

(C) Cumulative distributions of dendrite territories of horizontal cells in wild-type ( $4,455 \pm 478 \mu\text{m}^2$ ,  $n = 11$  cells,  $n = 3$  retinas) and *Amigo2* KO ( $4,523 \pm 441 \mu\text{m}^2$ ,  $n = 13$  cells,  $n = 4$  retinas) mice.  $P = 0.91$  by Mann-Whitney U test.

(D and E) Maximum intensity projections of horizontal cell axons labeled by AAV-CAG-YFP in wild-type (D) and *Amigo2* KO (E) mice.

(F) Cumulative distributions of axon territories of horizontal cells in wild-type ( $7,899 \pm 571 \mu\text{m}^2$ ,  $n = 14$  cells,  $n = 4$  retinas) and *Amigo2* KO ( $7,145 \pm 302 \mu\text{m}^2$ ,  $n = 23$  cells,  $n = 4$  retinas) mice.  $P = 0.24$  by Mann-Whitney U test.

Throughout the figure, ns indicates no significant differences for statistical comparisons.

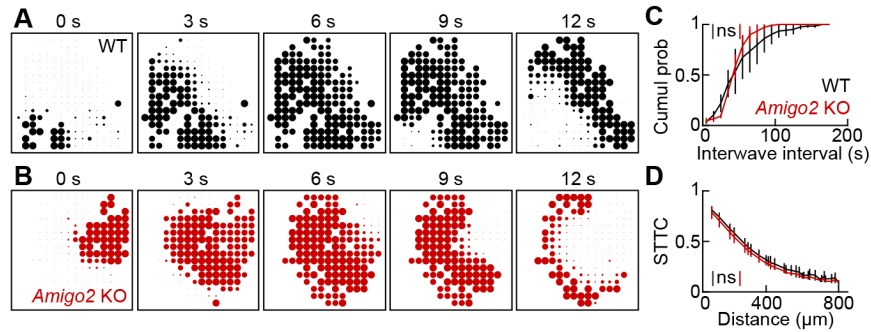


**Figure S6. Cholinergic waves in wild-type and *Amigo2* KO retinas** (related to Figure 6)

(A and B) Representative cholinergic waves recorded in P7 wild-type (A) and *Amigo2* KO (B) retinas. Each square represents the activity of ganglion cells recorded on a multielectrode array. Activity is proportional to the size of the filled circles.

(C) Cumulative distributions of the interwave intervals in wild-type ( $n = 152$  cells,  $n = 2$  retinas) and *Amigo2* KO ( $n = 110$  cells,  $n = 2$  retinas) mice.  $P = 0.44$  by bootstrapping.

(D) Spike time tiling coefficients (STTCs) for cell pairs plotted as a function of cell-cell distances were not significantly different between wild-type ( $n = 32,530$  pairs,  $n = 2$  retinas) and *Amigo2* KO ( $n = 23,906$  pairs,  $n = 2$  retinas) mice.  $P = 0.54$  by bootstrapping.

Throughout the figure, ns indicates no significant differences for statistical comparisons.